

HIGH CURRENT PROTON BEAM INVESTIGATIONS AT THE SILHI-LEBT AT CEA/SACLAY

R. Hollinger, W. Barth, L. Dahl, M. Galonska, L. Groening, P. Spaedtke, GSI, Darmstadt, Germany
O. Meusel, IAP, Frankfurt, Germany
R. Gobin, P. A. Leroy, CEA, Saclay, France

Abstract

The future proton LINAC at GSI for FAIR requires that the ion source and the low energy beam transport system deliver a 100 mA proton beam with an energy of 95 keV within an acceptance of 0.3π mm mrad (normalized, rms) at the entrance of the RFQ. Between the ion source and the RFQ a 2-solenoid focussing system is foreseen. The beam parameters of the present SILHI ion source (Source d'Ions Légères a Haute Intensités) and its 2-solenoid LEPT setup at CEA/Saclay generally meet these requirements. This represents a unique possibility to investigate the injection of a high current proton beam into a low energy beam transport system under the influence of space charge with conditions similar to those required in the future at GSI. Therefore, measurements on various beam parameters have been performed at the end of the SILHI LEPT system by a CEA/IAP/GSI collaboration. Results of these measurements reveal that a proton current of 100 mA can be achieved but the emittance is as high as $0.4-0.5 \pi$ mm mrad (95 %, normalized, rms).

INTRODUCTION

In the framework of the GSI future project FAIR (Facility for Antiproton and Ion Research) [1], a new proton injector is planned to serve the existing synchrotron SIS18 with up to 70 mA of protons at 70 MeV [2]. The LINAC consists of an ion source producing 100 mA at 95 keV, a short 2-solenoid LEPT, a 4-rod 3 MeV RFQ, and 12 crossed bar H-cavities.

The ECR ion source SILHI and the LEPT system at CEA/Saclay [3,4] generally meet our requirements. Tab. 1 gives an overview of the design parameters at the end of the LEPT system compared to present SILHI parameters.

Table 1: Beam Parameters

	Required	SILHI
H⁺ current	100 mA	105 mA**
Full beam	<115 mA	110 mA**
Energy	95 keV	95 keV
Duty cycle	4 Hz	4 Hz
Pulse length	>36 μ s	>300 μ s**
Emittance*	0.3π mm mrad	$\leq 0.5 \pi$ mm mrad**
Noise	< ± 5 %	± 7 %**
Life time	months	months
Availability	>90 %	99 %

*(norm., rms), **(typical values, not optimized for pulsed operation)

A collaboration with CEA provided a unique opportunity to study the ion beam behaviour for different

settings of the LEPT and different boundary conditions, including modified residual gas pressure. Beam emittance measurements with a high-resolution slit-grid measurement device were carried out as well as space charge compensation measurements using a 4-grid analyzer [5,6]. Beam emittance measurements as such as measurements of the space charge compensation for different settings of the solenoids was the main topic of the investigation program.

EXPERIMENTAL SETUP

The SILHI ion source was developed in the 90's for a cw H⁺ beam, but the source is also able to run in a pulsed mode by pulsing the rf generator. The ion source operates with a frequency of 2.45-3 GHz. A well designed pentode system allows high brightness ion beams with energies of up to 100 keV and full beam currents of 130 mA [3,4,7].

For the emittance measurements the timing of the ion source has been set to 4 Hz repetition rate and 0.6 ms pulse length. The low duty cycle of the ion source results in a proton fraction of 95 % and 5 % H₂⁺. This is a 5 % higher proton fraction compared to the cw mode.

Generally, the LEPT consists of two 0.5 m long solenoids ($B_{\max} = 260$ mT) and two magnetic steerers to adjust the horizontal and vertical beam position. In addition, beam transformers and Faraday cups are installed to measure the ion beam intensity close behind the pentode system, between the solenoids, and at the end of the beam line. A Wien filter allows detection of differing ion species as a check of beam purity. Fig. 1 shows a schematic drawing of the LEPT.

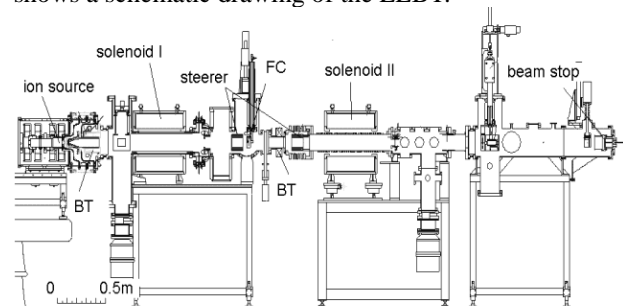


Figure 1: Schematic drawing of the SILHI-LEBT [7].

The slit of the emittance measurement device was installed 0.9 m behind the second solenoid. Tab. 2 presents all relevant data of the emittance measurement device.

Table 2: Parameters of the Slit-Grid Measurement Device

Slit	0.1 mm x 60 mm
Grid	60 wires, 0.1 mm x 80 mm
Resolution in space	0.25 mm
Resolution in angle	0.5 mrad
Max. detected angle	120 mrad

The measurements are divided into the following tasks:

- Emittance as a function of the flux density of solenoid II for a parallel beam behind solenoid I, $B_{sol I} = 129$ mT (Case I)
- Emittance as a function of the flux density of solenoid II for a focused beam behind solenoid I, $B_{sol I} = 200$ mT (Case II)
- Emittance for a beam which is matched to the acceptance of the RFQ (large convergence angles)
- Emittance for a higher residual gas pressure
- Space charge measurements with a 4-grid-analyzer

For all the emittance measurements only the vertical plane was analysed. The ion beam is assumed to be rotationally symmetric.

EXPERIMENTAL RESULTS

Although the ion source was not optimized for pulsed operation, the rise time of the beam pulse as well as the level of beam noise and fluctuations are acceptable. Fig. 2 shows a typical current signal at the beam dump.

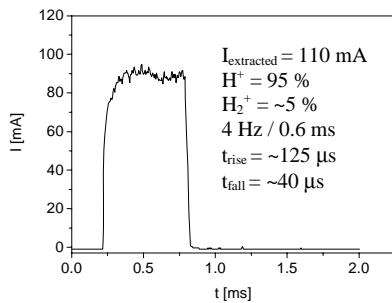


Figure 2: Typical ion current signal at the beam dump.

Emittance as a Function of Solenoid II Excitation for a Parallel Beam behind Solenoid I (Case I)

For the transport of an ion beam through a two-solenoid LEBT system, the best choice is to set the first solenoid to a level where the preferred ion species is transported parallel through the first solenoid. The second solenoid focuses the ion beam into the following rf accelerator. This was the first scenario which has been investigated. Solenoid I was set to 129 mT for a nearly parallel proton beam and solenoid II was varied from 29 to 200 mT. Fig. 3 presents the emittance patterns for 29 mT (a), 86 mT (b), 143 mT (c), and 200 mT (d).

In Fig. 3a protons and molecules (H_2^+) are slightly separated and small aberrations are visible. Fig. 3b shows well-separated protons and stronger aberrations. Additionally, one can see a pattern forming in the centre,

which is called ‘satellites’ in the following. A focused proton beam is presented in case (c). Here the satellites increase, whereas the molecules are well separated. Although the focussing strength is increased from (b) to (c) the satellites have the same twiss parameter α . Only the divergence angle and the diameter are changing. The aberrations of the proton beam are not increasing. This gives a slight hint that the filamentation is not space charge dominated. In Fig. 3d the proton beam is free of aberration and well focused. The satellites are covered by the proton beam.

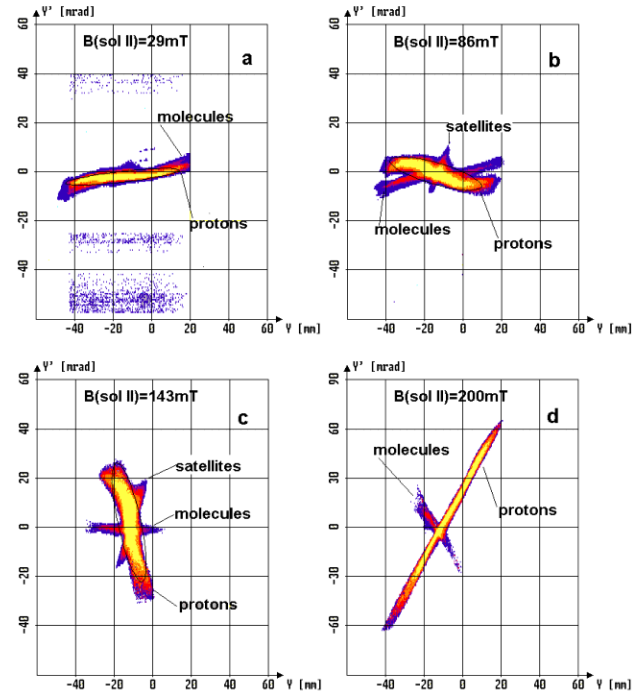


Figure 3: Emittance patterns for Case I where protons leave solenoid I nearly parallel, $B_{sol I} = 129$ mT.

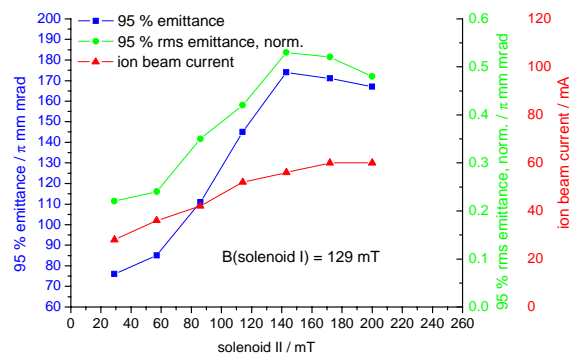


Figure 4: Beam emittance and current at the beam dump as a function of the flux density of solenoid II with $B_{sol I} = 129$ mT.

Fig. 4 summarizes the evaluation of the emittance and beam current for Case I ($B_{sol I} = 129$ mT). Solenoid II varies from 29 to 200 mT. For the given emittances only the proton fraction was taken into account.

The total emittance increases by a factor of 2.3 (rms-emittance by a factor of 1.7) with increasing flux density of solenoid II. Although the emittance pattern for $B_{\text{solenoid II}} = 200$ mT shows nearly no filamentation, the value of the emittance is relatively high (Fig. 3d). Neither space charge effects nor aberrations due to misalignment can be made clearly responsible. It seems that both are contributing to emittance growth. If the flux density exceeds the 200 mT value the emittance becomes smaller because the pattern gets very narrow. However, the ion beam current at the beam dump shows a maximum of 60 mA for 200 mT.

Emittance as a Function of Solenoid II Excitation for a Focused Beam behind Solenoid I (Case II)

In a second step solenoid I was set to 200 mT, whereas solenoid II has been varied from 0 to 260 mT. In this case the ion beam passes through a focus 18 cm in front of solenoid II. Here the transmission through the whole LEBT was optimal, resulting in ion beam currents of up to 108 mA at the beam dump.

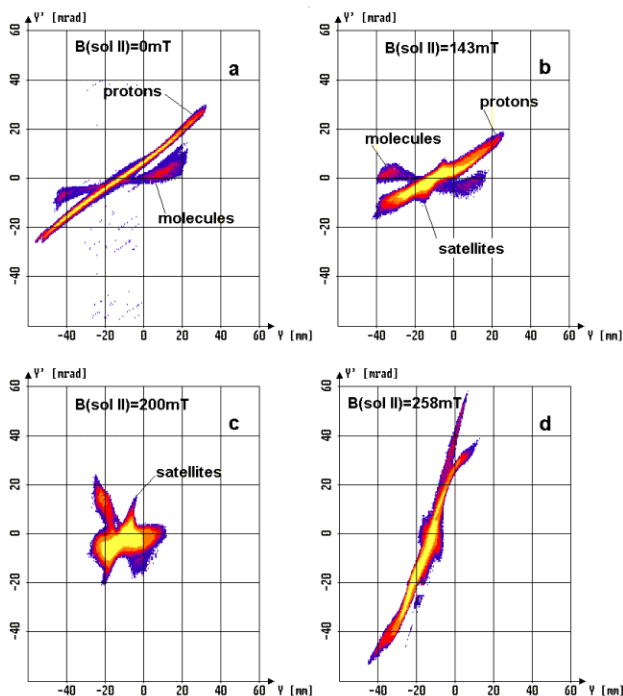


Figure 5: Emittance patterns for Case II where protons leave solenoid I focused, $B_{\text{solenoid I}} = 200$ mT.

Fig. 5 presents selected emittance patterns for different flux densities of solenoid II.

Emittance pattern (a) shows a well separated proton beam. The ion beam is divergent and indicates less aberrations. The phase space distribution indicated a hollow beam for H_2^+ . A second population arises close to the protons (bottom left). This population is not identical with the satellite known from Case I, which becomes obvious noting Fig. 5b. Here the satellites are more prominent, and the second population disappears. A

further increase of solenoid II leads to the best transmission through the LEBT. The ion beam current at the end of the beam line was 108 mA. This is in coherence with the small divergence angles of Fig 5c. The ion beam became asymmetric; all ion species are mixed. This suggests a misalignment of the solenoids. A further increase of solenoid II results in a divergent ion beam with strong aberrations (Fig 5d).

Fig. 6 summarizes the results: The total emittance as well as the rms-emittance increases with rising flux density by a factor 2, and 1.6, respectively. The asymmetric phase space distribution behind solenoid II (when solenoid II is on) as well as the misalignment causes significant emittance growth. However, the emittance for a focused beam is not higher as for a parallel beam behind solenoid I (see Fig. 4) although the ion beam is more symmetric for Case I. The maximum ion beam current for Case II is a factor of 1.8 higher compare to Case I. As a consequence the rms-beam brilliance for Case II is a factor of 2.6 higher.

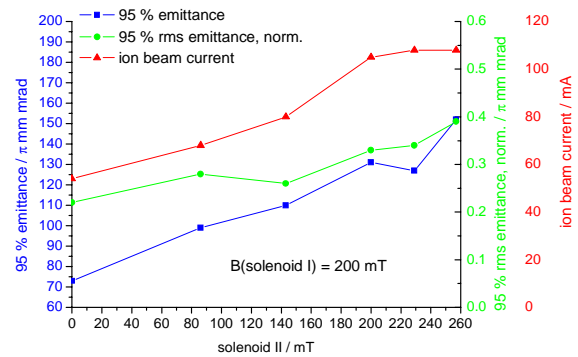


Figure 6: Beam emittance and current as a function of the flux density of solenoid II with $B_{\text{solenoid I}} = 200$ mT.

Emittance for RFQ Injection

The emittances shown for Cases I and II are not suitable for the injection into the RFQ because the divergence/convergence angles are too small. Therefore, they are increased with a further increase of solenoid II for Case I. Fig. 7 shows the emittance pattern. Solenoid I was set to 129 mT, solenoid II to 215 mT. The ion beam now is focused 20 cm in front of the slit. The divergence angles are ± 75 mrad, which seems comfortable for the RFQ injection. Although the ion beam is divergent and not convergent as required for the RFQ acceptance, one can transform it back without objection. The value of the emittance behind a focus is always higher than or equal to that in front of the focus, if space charge effects are taken into account. Compared to the emittances shown before, the molecules H_2^+ and H_3^+ as well as the neutrals are well separated. The satellites are still present but covered by the protons. The total emittance is 344π mm mrad, if all species are taken into account, the normalized rms-emittance amounts to 2.7π mm mrad. Considering only the proton beam, the total emittance decreases dramatically to 170π mm mrad ($\epsilon_{\text{rms},n} = 0.48 \pi$ mm mrad).

However, the value is still 60 % above the acceptance of the RFQ. Fig. 7 (right) shows the simulated phase space distribution which is in a very good agreement with the measurement. The 90 % rms-emittance is 0.2π mm mrad. Inside the solenoids a compensation of 80 % and outside of 100 % was considered. The beam compensation has been taken into account by using the “net current method” [8].

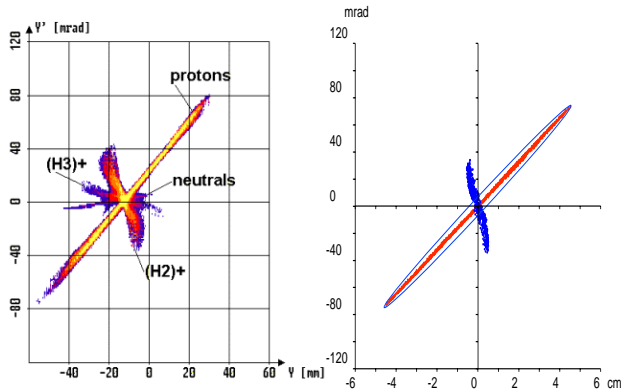


Figure 7: Emittance patterns for the RFQ injection. Left: Measurement, right: Kobra3-INP simulation

Emittance at a Higher Residual Gas Pressure

Due to the fact that the emittance is too high in combination with aberrations and space charge effects, the emittance could be reduced with a higher residual gas pressure.

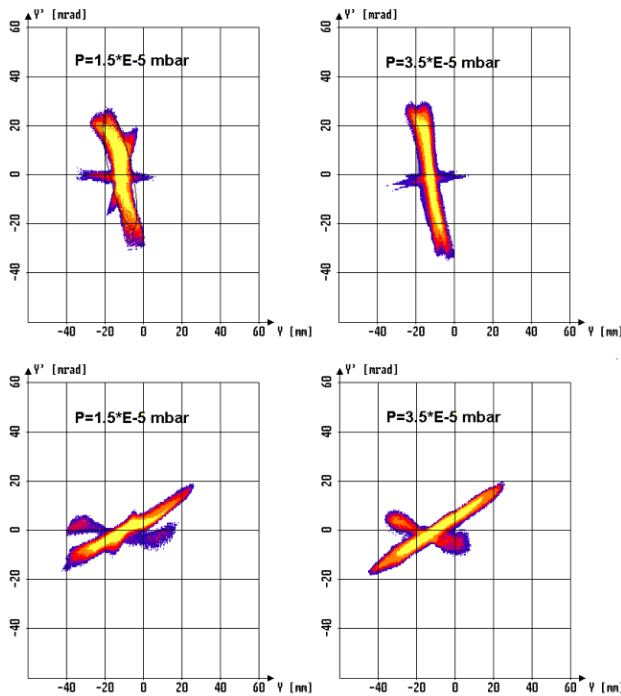


Figure 8: Emittance patterns for a higher residual gas pressure N_2 (right), $B_{sol II} = 143$ mT. Top: parallel beam behind solenoid I, bottom: focussed beam behind solenoid I.

An increase of the residual gas pressure leads to an increase of the secondary electron density in the beam channel. If the ion beam is dominated by space charge effects due to a too low secondary electron density, the emittance should be smaller with higher residual gas pressure. Nitrogen as background gas was injected between the solenoids. The pressure was increased from 1.5 to $3.5 \cdot 10^{-5}$ mbar for Case I and II. As a result the emittance as well as the shape of the emittance changed significantly as presented in Fig. 8. The emittances are presented with low residual gas pressure for the parallel beam and the focused beam behind solenoid I. Solenoid II was set to 143 mT in both cases. The rms-value of the emittance is up to 20 % smaller and the emittance patterns are well shaped with smaller aberrations. In addition the satellites and the hollow beam for H_2^+ disappears. This indicates that the satellites were generated because the secondary electron density was too low, or the density distribution was not homogenous in radial direction.

Space Charge Compensation Measurements with a 4-Grid-Analyzer

The emittance behaviour of the beam as shown before can be explained by aberrations and space charge effects. Therefore, a 4-grid-analyzer had been used to measure the beam potential between the two solenoids and behind the second solenoid for different settings of the solenoids.

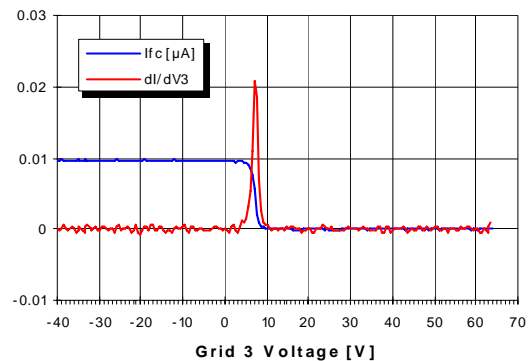


Figure 9: Secondary ion beam current and its derivative for a 100 mA proton beam, measured with a 4-grid-analyzer. I_{FC} : Faraday cup current as function of the grid voltage V_3 , dI/dV_3 : Derivative of the signal.

A variation of solenoid I between 0 mT and 172 mT does not lead to a change of the beam compensation. It is in a range of 95-96 %. A typical curve for the ion intensity measured with the 4-grid-analyzer and its derivation is shown in Fig. 9. For the evaluation of the space charge compensation value, the half height width of the derivative as well as the potential drop of beam edge and axis of a fully uncompensated ion beam was taken into account [9]. The 100 mA ion beam shows a degree of compensation of 96 %. Solenoid I was set to 143 mT to get a nearly parallel ion beam. If solenoid I was off or set to a high value (where ion beam losses were occurring) the compensation is >96 %. In this high-loss case, enough

secondary electrons are generated to ensure nearly full compensation.

With an increased residual gas pressure ($3.8 \cdot 10^{-5}$ mbar, N_2) the level of beam compensation was up to 99 % even for the 100 mA case. In addition, the derivative of the measured curve gets narrower, which means that the potential drop between beam edge and beam axis is smaller.

Measurements with the 4-grid-analyzer behind solenoid II shows a lower degree of compensation for all Cases. The value is in the range of 85-95 %. The ion beam needs a certain time to retrieve the high level of beam compensation. Compare to the measurements behind solenoid I the 4-grid-analyzer was installed much closer to solenoid II.

DISCUSSION

It seems that inside the solenoids space charge compensation of the ion beam is reduced, while outside the beam is nearly fully compensated. However, the emittance is dominated by the solenoids and not by the pentode system of the ion source. Inside the solenoids the electrons are not able to move in radial direction with the same mobility as outside. Additionally, electrons are confined to the axis of the solenoids. Secondary electrons which are generated close to the fringe field because of beam losses are moving towards the axis.

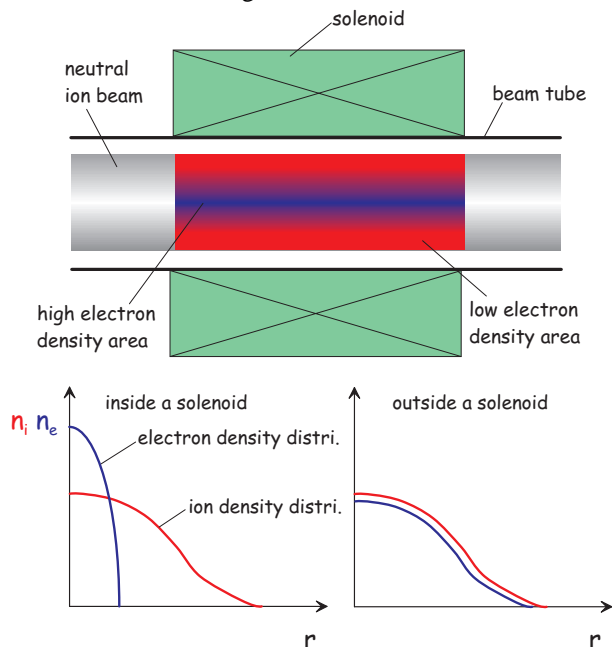


Figure 10: Particle density distribution inside and outside of a solenoid. Electron and ion density distribution inside and outside of a solenoid as a function of the radius.

As a result the electron density at the beam axis is very high, whereas the density outside is rather low. The net effect is an overcompensation in the middle of the beam and less compensation on the edges. The overcompensated part of the beam has a diameter of about 10 mm and focuses the beam. The satellites are generated

in this part of the beam [10]. Computer simulations with KOBRA3-INP [8] have shown that the focussing strength due to the overcompensation is analogue a solenoid with 250 mT. This is the reason why the α of the satellites does not change much with a variation of the focussing strength of the solenoids. Fig. 10 presents a schematic drawing of the electron density distribution inside and outside the solenoids.

With an increased residual gas pressure the situation relaxes. The density distribution inside the solenoids becomes more homogenous. The aberrations in the emittance pattern decrease with higher residual gas pressure, the ion beam inside the solenoid is compensated to a higher degree.

However, with shorter solenoids the space charge forces are reduced and we will obtain emittances suitable for the RFQ.

ACKNOWLEDGMENTS

The authors are grateful to U. Ratzinger (IAP-Frankfurt) for the item on loan of parts of the emittance measurement devices and to R. Boywitt and F. Peldzinski (GSI) for the help during the measurements and preparation of the emittance scanner. The authors would also like to thank all the IPHI group members for their technical assistance and participation in fruitful discussions.

REFERENCES

- [1] FAIR, Baseline Technical Report, Vol. 2, Accelerator and Scientific Infrastructure, 2006.
- [2] L. Groening et al., "The 70 MeV Proton Linac for the Antiproton and Ion Research FAIR", these proceedings.
- [3] R. Gobin et al., "High Intensity ECR Ion Source Developments at CEA/Saclay" RSI, Vol. 73, No. 2, p. 922, 2002.
- [4] R. Gobin et al., "Status of the Light Ion Source Developments at CEA/Saclay" RSI, Vol. 75, No. 5, p. 1414, 2004.
- [5] R. Ferdinand et al., "Space Charge Neutralization Measurement of a 75 keV, 130 mA Hydrogen Ion Beam" IEEE, 1998.
- [6] J. Sherman et al., "H⁺ Beam Neutralization Measurements with a Gridded Energy Analyzer, a Non-Interceptive Beam Diagnostic" LINAC 1988, p. 155, 1988.
- [7] J. M. Langniel et al. "Status and New Developments of the High Intensity Electron Resonance Source Light Ion Continuous Wave, and Pulsed Mode" RSI, Vol. 71, No. 2, p. 830, 2000.
- [8] M. Galonska et al. "Computer Simulations of a High Current Proton Beam at the SILHI-LEBT", these proceedings.
- [9] P. Kreisler et al., "Measurements of Space Charge Compensation of Ion Beams", Vacuum 34 (1-2), p. 215, 1984.
- [10] P. Groß, Thesis, Frankfurt, 2000.